Available online at www.sciencedirect.com
SCIENCE DIRECT®
Journal of Power Sources 119–121 (2003) 654–657
JOURNAL OF POWER SOURCES
www.elsevier.com/locate/jpowsour

First-principles calculations on Li_xNiO_2: phase stability and monoclinic distortion

M.E. Arroyo y de Dompablo*, G. Ceder

Department of Material Science and Engineering and Center for Materials Science and Engineering, Massachusetts Institute of Technology, Cambridge, MA 02139, USA

Abstract

The phase diagram of Li_xNiO_2 ($0 < x < 1$) and the evolution of the monoclinic distortion as a function of the lithium content are calculated using a combination of first-principles energy methods and statistical–mechanics techniques. As a function of the temperature different ordered Li_xNiO_2 structures appear in the phase diagram at $x = 0.25$, 0.33, 0.4, 0.5 and 0.75. Noteworthy, a new and unsuspected phase, $Li_{0.4}NiO_2$, dominates the low-lithium region of the phase diagram. In agreement with experimental results, maxima in monoclinicity (a_m/b_m) are predicted to occur near $Li_{0.75}NiO_2$ and $Li_{0.4}NiO_2$. The coupling between the Li-vacancy ordering and the Jahn–Teller activity of Ni^{3+} ions plays a crucial role in the stability of ordered Li_xNiO_2 structures and is at the origin of the monoclinic distortion. As a result, the different electrochemical behavior of Li_xNiO_2 versus Li_xCoO_2 lies in the electronic nature of the involved transition metal cation.

Keywords: First principles; $LiNiO_2$; Lithium intercalation; Battery material

1. Introduction

$LiNiO_2$ has been the focus of significant attention due to its potential application as electrode in lithium batteries [1]. Its structure (see Fig. 1) can be viewed as an ''ordered rock salt'' in which alternate layers of Li^+ and Ni^{3+} ions occur in octahedral sites within the *ccp* oxygen array, making up a rhombohedral structure [2]. $LiNiO_2$ is isostructural with $LiCoO_2$, the compound mostly used as positive electrode in rechargeable lithium batteries, though they behave fundamentally different. The Li_xCoO_2 system is well characterized [1], whereas in Li_xNiO_2 the sequence of phase transitions and ordered Li_xNiO_2 structures that occurs during the lithium intercalation/deintercalation is still unclear [1,3–7]. It is assumed that in the range $0.75 < x < 1$ the rhombohedral symmetry of the starting compound is maintained. Between $Li_{0.5}NiO_2$ and $Li_{0.75}NiO_2$ a monoclinic region has been claimed to occur, and for compositions below $Li_{0.3}NiO_2$ a rhombohedral symmetry is stable. Ordered structures have been proposed at $Li_{0.25}NiO_2$ [1,5], $Li_{0.33}NiO_2$ [1], $Li_{0.5}NiO_2$ [1,5,8,9], $Li_{0.63}NiO_2$, [1,9] and $Li_{0.75}NiO_2$ [1,5,9], though experimental evidence has been reported only at $x = 0.25$, 0.33 and $Li_{0.63}NiO_2$ [1,9].

Despite the potential Jahn–Teller (J–T) activity of Ni^{3+} cations, $LiNiO_2$ adopts rhombohedral symmetry in the R-3m space group at any temperature [10]. Removal of lithium from $LiNiO_2$ leads to monoclinic phase Li_xNiO_2 with $0.4 < x < 0.75$ [1,3,4,9]. The origin of this large monoclinic region is controversial. One possible and obvious driving force is a cooperative distortion of NiO_2 octahedra [3,5,11] due to the Jahn–Teller effect of trivalent nickel ions. However, as has been claimed by some authors [1,9], this cause of the monoclinicity is somewhat unlikely: since a cooperative J–T distortion is not present in $LiNiO_2$, it is unlikely that a material with a lower concentration of J–T distorted Ni^{3+} octahedra could have a collective J–T distortion. Since lithium removal also creates vacancies, Li-vacancy ordering can take place. Hence, it has been speculated that such Li ordering may be the cause of the monoclinic distortion in partially delithiated Li_xNiO_2 [1,9].

As a first-principles calculation gives detailed information on the local structure as function of composition, it may be useful to further clarify the phase diagram of Li_xNiO_2 as well as the origin of the monoclinic distortion. First-principles refers to the use of quantum mechanics to determine the structure or properties of materials at 0 K. A combination of first-principles total energy calculations and statistical–mechanics allows to obtain finite-temperature thermodynamic properties. Here we report on the phase stability of Li_xNiO_2 as a function of concentration and temperature, and

* Corresponding author. Present address: CIDETEC, Paseo de Mikeletegi 61, San Sebastian 20009, Spain.
E-mail address: earroyo@cidetec.es (M.E. Arroyo y de Dompablo).

0378-7753/03/$ – see front matter © 2003 Elsevier Science B.V. All rights reserved.
doi:10.1016/S0378-7753(03)00199-X

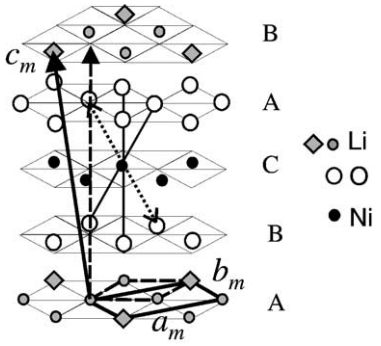

Fig. 1. Schematic representation of the $LiNiO_2$ structure. Lithium ions in planes A and B are denoted with solid gray circles and diamonds. The diamonds are those Li ions that are at the extension of the Ni–O bond forming 180° Li_A–O–Ni^{3+}O–Li_B complexes. The cell with rhombohedral symmetry in the hexagonal setting is indicated by dashed lines. An hypothetical distortion of the Ni–O octahedra due to J–T effect is indicated by a dotted line, with the basic monoclinic cell indicated by bold lines.

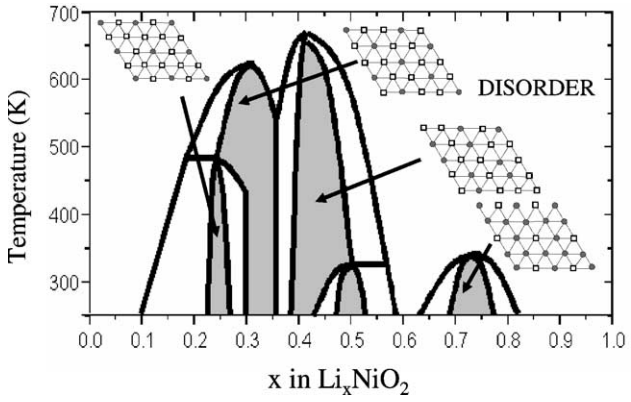

Fig. 2. Calculated phase diagram of Li_xNiO_2. The gray areas represent ordered Li_xNiO_2 regions. The insets show the Li-vacancy distribution in the ordered structures stable at room temperature. Li ions are denoted by circles and vacancies by squares.

examine the evolution of the monoclinic distortion with the lithium content at room temperature. We will show that the particular behavior found in Li_xNiO_2 is related to the Jahn–Teller activity of Ni^{3+} ions coupled to the Li-vacancy ordering.

2. Method

The theoretical background to obtain a phase diagram from first-principles calculations can be found in some of our previous work [12–14]. The methodology followed in the Li_xNiO_2 system for the phase diagram and monoclinicity is detailed in [14–16].

3. Results

3.1. Phase diagram

During the cycling of a lithium cell the lithium ions are reversibly removed from and reinserted into Li_xNiO_2 creating or annihilating vacancies within the triangular lithium planes. Li-vacancy ordered structures can appear at several characteristic Li compositions depending on the relative magnitude of the first, second and further neighbor's interactions [13,17]. In a first-principles study of the Li_xCoO_2 system [12], we found the interactions between Li ions to be mainly repulsive and decaying with distance, as they are likely determinate by screened electrostatics and some oxygen displacement. In layered $LiMO_2$ different lithium planes are relatively far apart (∼ 5 Å) and are separated by the transition-metal layer, so in principle no important interlayer Li–Li interactions are expected, as was found in Li_xCoO_2 [12,13]. Contrary to this, in Li_xNiO_2 non-negligible attractive interactions exist between Li ions in different planes [14,16]. In particular we found that the interaction between Li ions that are on the extensions of linear O–Ni–O bonds is crucial for stabilizing some of the ordered ground states in the phase diagram [14]. In a comparative study [16], we found that all Li_xNiO_2 structures with such 180° Li_A–O–Ni–O–Li_B configurations have lower energy than structures without these configurations but with the same in-plane lithium ordering.

Fig. 2 shows the calculated equilibrium phase diagram for Li_xNiO_2. Ordered structures of lithium ions and vacancies appear at Li_xNiO_2 with $x = 0.25$, 0.33, 0.4, 0.5 and 0.75 (gray regions in Fig. 1). These ordered regions are separated by domains of two-phase coexistence. At room temperature all phase transitions detected in this system are first order. Fig. 3 shows the predicted most stable Li-vacancy distribution at several ordered compositions. The most stable Li-vacancy arrangements for $Li_{0.25}NiO_2$ and $Li_{0.33}NiO_2$ in

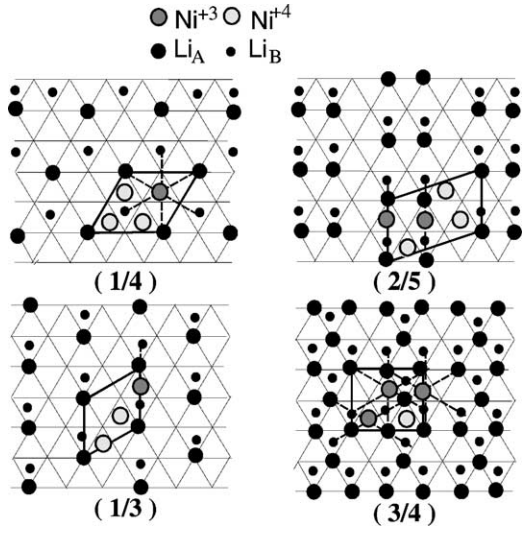

Fig. 3. Lowest energy Li-vacancy arrangements in Li_xNiO_2 at x values of 0.25, 0.33, 0.4 and 0.75. The big black circles denote the in-plane lithium orderings and the small black circles designate the positions of the Li ions in the adjacent plane. Dashed line indicates the 180 Li–O–Ni^{3+}O–Li configurations (see Fig. 1). Ni^{3+} ions are indicated by dark gray circles and Ni^{4+}ions by light gray circles.

the calculations agree with the experimental models from selected area electron diffraction data (SAED) [1]. We furthermore predicted particular ordered configurations at compositions $Li_{0.75}NiO_2$ and $Li_{0.5}NiO_2$, where a different ordering has been postulated [1,8,9] but no experimental characterization has been performed. In the region $0.5 < x < 0.75$ first-principles calculations do not agree with the model proposed by Peres et al. to explain the ordered structure found by SAED in a sample of nominal composition $Li_{0.63}Ni_{1.02}O_2$ [9]. At $Li_{0.4}NiO_2$ we predict a stable phase with rows of nearest neighbors dumbbells. While this phase dominates the phase diagram at low-lithium concentration, it has not been considered in any previous work. Notice that at each composition the lowest energy structures gives a relation between ordering in successive planes so that Li–Li or vacancy–vacancy pairs exist along the O–Ni^{3+}O extensions, but never a Li–vacancy pair. These Li_A–O–Ni^{3+}O–Li_B complexes are shown by the dotted lines in Fig. 3.

The calculated phase diagram corresponds to stoichiometric $LiNiO_2$. However, in $LiNiO_2$ some departure from stoichiometry is unavoidable, and a compound $Li_{1-z}Ni_{1+z}O_2$ is obtained [1]. The introduction of some disorder in $LiNiO_2$ will decrease the temperature of the order–disorder transitions. The disorder introduced by the Ni excess can also affect the character of the phase transformations.

3.2. Monoclinic distortion in Li_xNiO_2

In a monoclinic cell a measure of the departure form the rhombohedral symmetry is given by the ratio between the a and b monoclinic lattice parameters, a_m/b_m (see Fig. 1). In an undistorted rhombohedral structure, this value would be $\sqrt{3}$. Following the methodology detailed in [15] we have calculated the evolution of the monoclinicty a_m/b_m with the composition at room temperature. This result is shown in Fig. 4. Experimental data taken from Li et al. [4] are also plotted for comparison. In the region where experimentally monoclinicity is observed ($0.4 < x < 0.75$) the monoclinicity varies considerably as the stable Li-vacancy ordering varies with composition. The calculated a_m/b_m value decreases slightly in the range $1 < x < 0.8$. Then around $Li_{0.75}NiO_2$ there is a maximum, followed by a drop in the monoclinicity. A second maximum appears near $Li_{0.4}NiO_2$. The calculated data in Fig. 4 are in qualitative agreement with the experimental data. However, some quantitative discrepancies in composition and magnitude between the experimental and calculated monoclinicity maxima seems to be present. This is likely due to the fact that experiments are always performed on non-stoichiometric $Li_{1-z}Ni_{1+z}O_2$ [1].

We have previously reported that in Li_xNiO_2, lithium ordering couples to orbital and Jahn–Teller ordering so as to produce long-range attractive interaction between Li ions in different planes [16]. In the previous section, we have shown that this 180 Li_A–O–Ni^{3+}O–Li_B complexes are present in all the most stable Li_xNiO_2 structures. We review how the monoclinic distortion arises because of this unusual

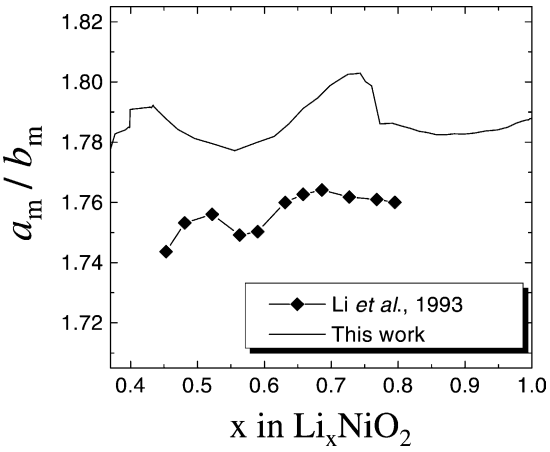

Fig. 4. Calculated variation of a_m/b_m vs. x in Li_xNiO_2 at room temperature. Experimental data taken from [4] are also plotted for comparison.

synergetic effect between the Li-vacancy ordering and the Jahn–Teller activity of Ni^{3+}.

In an octahedral environment, the five d orbitals of a transition metal atom split in two groups; the t_{2g} group (d_{xy}, d_{yz}, d_{xz}) pointing away from oxygen atoms, and the e_g group ($d_{x^2-y^2}$, d_{z^2}). The latter overlap directly with the p_x, p_y and p_z oxygen orbitals forming bonding e_g bands and antibonding e_g^* bands. The antibonding e_g^* bands are predominantly d in character, and lie above the t_{2g} bands. Each oxygen at the vertex of M octahedral is also connected through the $2p_x$, $2p_y$ and $2p_z$ orbitals to the 2s orbital of a lithium ion, so that one of these lithium ions is "sharing" an O 2p orbital with M (see Fig. 8 in [16]). These Li 2s orbitals, oxygen 2p and metal e_g^* orbitals have the proper symmetry to hybridize. When the transition metal has empty e_g^* orbitals, as is the case in $LiCoO_2$, the hybridization of the e_g^* orbitals with Li 2s orbitals will not affect the energy. However, in Li_xNiO_2 the presence of Li ions at the extension of a Ni–O bond lowers the energy of that filled Ni e_g^* orbital. Since the energy of Jahn–Teller distortion is largest when charge is localized in completely filled spin orbitals, Li ions will preferentially hybridize with the same e_g^* orbital. This leads to attractive inter-planar Li interactions whenever those Li ions hybridize with the same e_g^* orbital, i.e. whenever they form a 180° Li_A–O–M–O–Li_B configuration. As we showed in the previous section, these interactions are crucial in the stability of ordered Li_xNiO_2 structures. Furthermore, the lining up of Li along one or two octahedral axis around Ni^{3+}, with vacancies along the other one, produces a remarkably stable and Jahn–Teller distorted configuration. In this way, at $x = 0.4$ and 0.75 the stable Li orderings are particularly conducive to Jahn–Teller distortion, thereby creating two maxima in the monoclinicity. In $LiNiO_2$ all Li sites are filled and the Jahn–Teller distortion is not assisted by the Li-vacancy ordering. Therefore, the distortion is expected to be somewhat smaller in magnitude, giving only a weak (in calculations) or non-existent (in experiments) Jahn–Teller distortion.

4. Summary

We have performed a first-principles investigation of phase stability in stoichiometric Li_xNiO_2 for $0 < x < 1$, and analyzed the evolution of the monoclinic distortion as a function of the lithium content. The calculated results are in good agreement with experiments. We explain the stability of ordered Li_xNiO_2 structures and the monoclinic distortion by long-range attractive inter-plane Li–Li interactions related to the charge distribution and electronic structure of the Ni^{3+} ions. Therefore, the different electrochemical behavior found in isostructural Li_xNiO_2 and Li_xCoO_2 is due to the electronic nature of the involved M cations.

Acknowledgements

This work was supported by the Department of Energy under grant DE-FG02-96ER 45571. Support from the Singapore MIT Alliance is gratefully acknowledged. We express our sincere gratitude to C. Mariannetti and A. Van der Ven for insightful contributions to the work presented here. MEAD acknowledges support from Spanish MECD. GC acknowledges support from Union Minière in form of a Faculty Development Chair. NPACI resources were used for some of the computations in this work.

References

[1] C. Delmas, M. Menetrier, L. Croguennec, S. Levasseur, J.P. Peres, C. Pouillerie, G. Prado, L. Fournes, F. Weill, Int. J. Inorg. Mater. 1 (1999) 11.
[2] K. Mizushima, P.C. Jones, P.J. Wiseman, J.B. Goodenough, Mater. Res. Bull. 15 (1980) 783.
[3] T. Ohzuku, A. Ueda, M. Nagayama, J. Electrochem. Soc. 140 (1993) 1862.
[4] W. Li, J.N. Reimers, J.R. Dahn, Solid Sate Ionics 67 (1993) 123.
[5] H. Arai, S. Okada, H. Ohtsuka, M. Ichimura, J. Yamaki, Solid State Ionics 80 (1995) 261.
[6] A. Hirano, R. Kanno, Y. Kawamoto, Y. Takeda, K. Yamaura, M. Takano, K. Ohyama, M. Ohashi, Y. Yamaguchi, Solid State Ionics 78 (1995) 123.
[7] X.Q. Yang, X. Sun, J. McBreen, Electrochem. Commun. 1 (1999) 227.
[8] H. Arai, S. Okada, Y. Sakurai, J. Yamaki, Solid State Ionics 95 (1997) 275.
[9] J.P. Peres, F. Weill, C. Delmas, Solid State Ionics 116 (1999) 19.
[10] A. Rougier, C. Delmas, A.V. Chadwick, Solid State Commun. 94 (1995) 123.
[11] A. Hirano, R. Kanno, Y. Kawamoto, K. Oikawa, T. Kamiyama, F. Izumi, Solid State Ionics 86/88 (1996) 791.
[12] A. van der Ven, M.K. Aydinol, G. Ceder, G. Kresse, J. Hafner, Phys. Rev. B 58 (1998) 2975.
[13] G. Ceder, A. Van der Ven, Electrochim. Acta 45 (1999) 131.
[14] M.E. Arroyo y de Dompablo, A. van der Ven, G. Ceder, Phys. Rev. B 66 (2002) 064112.
[15] M.E. Arroyo y de Dompablo, G. Ceder, Chem. Mater. 15 (2003) 62.
[16] M.E. Arroyo y de Dompablo, C. Marianetti, A. van der Ven, G. Ceder, Phys. Rev. B 63 (2000) 144107.
[17] M. Kaburagi, J. Kanamori, J. Phys. Soc. Jpn. 44 (1978) 718.